Pyramid diffraction in parity-time-symmetric optical lattices

Sean Nixon and Jianke Yang*

Department of Mathematics and Statistics, University of Vermont, Burlington, Vermont 05401, USA
**Corresponding author: jyang@math.uvm.edu*

Received March 19, 2013; revised April 19, 2013; accepted April 24, 2013;
posted April 30, 2013 (Doc. ID 187442); published May 28, 2013

Nonlinear dynamics of wave packets in two-dimensional parity-time-symmetric optical lattices near the phase transition point are analytically studied. A fourth-order equation is derived for the envelope of these wave packets. A pyramid diffraction pattern is demonstrated in both the linear and nonlinear regimes. Blow-up is also possible in the nonlinear regime for both focusing and defocusing nonlinearities. © 2013 Optical Society of America

OCIS codes: (190.0190) Nonlinear optics; (160.5293) Photonic bandgap materials.
http://dx.doi.org/10.1364/OL.38.001933

Parity-time ($\mathcal{PT}$)-symmetric wave systems have the unintuitive property that their linear spectrum can be completely real even though they contain gain and loss [1]. In spatial optics, $\mathcal{PT}$-symmetric systems can be realized by employing symmetric index guiding and an antisymmetric gain/loss profile [2–5]. In temporal optics, $\mathcal{PT}$-symmetric systems can be obtained as well [6–8]. So far, a number of phenomena in optical $\mathcal{PT}$ systems have been reported, including phase transition, nonreciprocal Bloch oscillation, unidirectional propagation, distinct pattern of diffraction, formation of solitons and breathers, wave blow-up, and so on [4–14].

In this Letter, we analytically study nonlinear dynamics of wave packets in two-dimensional $\mathcal{PT}$-symmetric optical lattices near the phase transition point (where diffraction surfaces of Bloch bands cross like the intersection of four planes). Near these intersections we show that the evolution of wave packets is governed by a fourth-order equation. Based on this envelope equation, we predict a pyramid (i.e., expanding square) diffraction pattern in both linear and nonlinear regimes. Furthermore, in the nonlinear regime, blow-up can occur for both focusing and defocusing nonlinearities. These predictions are verified in the full equation as well.

The model for nonlinear propagation of light beams in $\mathcal{PT}$-symmetric optical lattices is taken as

$$i\Psi_z + \nabla^2\Psi + V(x,y)\Psi + \sigma|\Psi|^2\Psi = 0, \qquad (1)$$

where z is the propagation direction, (x,y) is the transverse plane, $\nabla^2 = \partial_x^2 + \partial_y^2$, and $\sigma = \pm 1$ is the sign of nonlinearity. The $\mathcal{PT}$-symmetric potential $V(x,y)$ is taken as $V(x,y) = \tilde{V}(x) + \tilde{V}(y)$, where

$$\tilde{V}(x) = V_0^2[\cos(2x) + iW_0\sin(2x)], \qquad (2)$$

V_0^2 is the potential depth, and W_0 is the relative gain/loss strength.

We begin by considering the linear diffraction relation of Eq. (1) at the phase transition point $W_0 = 1$ [9,13]. In this case, the linear Eq. (1) can be solved exactly [13]. The diffraction relation is $\mu = (k_x + 2m_1)^2 + (k_y + 2m_2)^2$, where (k_x, k_y) are Bloch wavenumbers in the first Brillouin zone $-1 \le k_x,\ k_y \le 1$, and (m_1, m_2) are any pair of nonnegative integers. The most complex degeneracies occur at points $k_x = 0, \pm 1$ and $k_y = 0, \pm 1$, where the diffraction surface intersects itself four-fold as illustrated in Fig. 1. If a carrier Bloch wave is chosen at one of these degeneracies, then the envelope of the resulting wave packet exhibits novel behavior, which we elucidate below.

The linear Eq. (1) for $\Psi = \phi(x,y)e^{-i\mu z}$ reduces to an eigenvalue problem $L\phi = -\mu\phi$, where $L = L^{(x)} + L^{(y)}$, $L^x \equiv \partial_x^2 + \tilde{V}_0 x$, and $\tilde{V}_0(x)$ is the $\mathcal{PT}$ lattice [Eq. (2)] at the phase transition point $W_0 = 1$. At the four-fold intersection points, the eigenvalues are $\mu = n_1^2 + n_2^2$, where (n_1, n_2) are any pair of positive integers. The operator $L^{(x)}$ ($L^{(y)}$) has eigenvalues n_1^2 (n_2^2) with geometric multiplicity 1 and algebraic multiplicity 2 [14]. Let $\phi^{e_1}(x)$ ($\phi^{e_2}(y)$) be the eigenfunction and $\phi^{g_1}(x)$ ($\phi^{g_2}(y)$) the associated generalized eigenfunction. Then,

$$\phi^{e_1}(x) = \tilde{I}_{n_1}(V_0 e^{ix}), \qquad \phi^{e_2}(y) = \tilde{I}_{n_2}(V_0 e^{iy}), \qquad (3)$$

where $\tilde{I}_n(V_0 e^{ix})$ is the modified Bessel function $I_n(V_0 e^{ix})$ normalized to have a unit peak amplitude, and

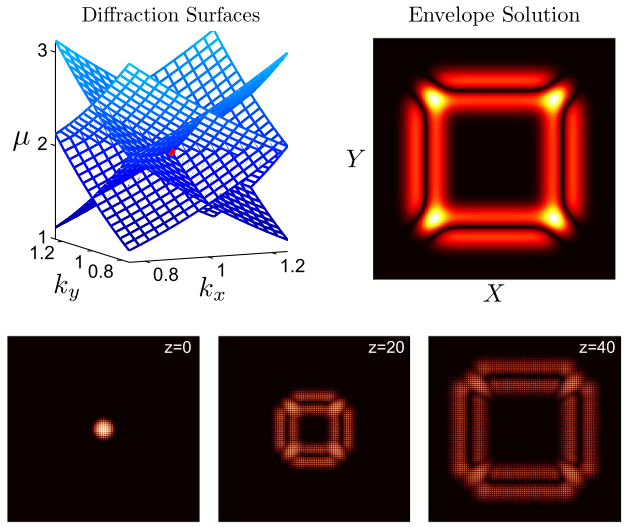

Fig. 1. (Upper left) Diffraction relation near intersection point $(k_x, k_y, \mu) = (1, 1, 2)$, marked by red dot. (Upper right) Linear diffraction of initial Gaussian envelope at phase transition in envelope Eq. (11). (Lower row) Linear diffraction of initial Gaussian wave packet at phase transition in full Eq. (1).

$(L^{(x)}+n_1^2)\phi^{g_1}=\phi^{e_1}$, $(L^{(y)}+n_2^2)\phi^{g_2}=\phi^{e_2}$. Since $L=L^{(x)}+L^{(y)}$, we see that L has two eigenfunctions

$$\phi^{01}(x,y)=\phi^{e_1}(x)\phi^{e_2}(y), \tag{4a}$$

$$\phi^{02}(x,y)=\phi^{e_1}(x)\phi^{g_2}(y)-\phi^{g_1}(x)\phi^{e_2}(y). \tag{4b}$$

In addition, the first eigenfunction ϕ^{01} has two generalized eigenfunctions

$$\phi^{11}(x,y)=[\phi^{e_1}(x)\phi^{g_2}(y)+\phi^{g_1}(x)\phi^{e_2}(y)]/2, \tag{5a}$$

$$\phi^{21}(x,y)=\phi^{g_1}(x)\phi^{g_2}(y)/2, \tag{5b}$$

where $(L+\mu)\phi^{11}=\phi^{01}$, and $(L+\mu)\phi^{21}=\phi^{11}$.

We now study the nonlinear dynamics of wave packets near these intersections. For simplicity, we will conduct the analysis at the lowest intersection point, $\mu=2$. The perturbation expansion for the wave packet near this point is

$$\Psi=\varepsilon^{\frac{3}{2}}\psi e^{-i\mu t},\qquad \psi=\psi_0+\varepsilon\psi_1+\ldots, \tag{6}$$

where $\psi_0=A(X,Y,Z)\phi^{01}(x,y)$ is the leading order wave packet for the Bloch mode ϕ^{01} at the intersection point $(k_x,k_y,\mu)=(1,1,2)$, $(X,Y,Z)=(\varepsilon x,\varepsilon y,\varepsilon z)$ are slow spatial variables, and $0<\varepsilon\ll 1$. Near the phase transition point, W_0 can be expressed as $W_0=1-\eta\epsilon^2/V_0^2$, where η measures the deviation from phase transition. After introducing the slow variables into Eq. (1), the new equation for ψ is

$$\begin{aligned}(L+\mu)\psi=&-i\varepsilon\psi_Z-2\varepsilon(\psi_{xX}+\psi_{yY})-\varepsilon^2(\partial_X^2+\partial_Y^2)\psi\\&+i\eta\varepsilon^2[\sin(2x)+\sin(2y)]\psi-\varepsilon^3\sigma|\psi|^2\psi.\end{aligned} \tag{7}$$

We proceed by inserting expansion Eq. (6) into Eq. (7) and solving for ψ_n at each order. Each ψ_n satisfies a linear inhomogeneous equation, with the homogeneous operator being $L+\mu$. In order for it to be solvable, the Fredholm conditions need to be satisfied, i.e., the inhomogeneous term must be orthogonal to the kernels ϕ^{01*} and ϕ^{02*} of the adjoint operator $L^*+\mu$. Here, $*$ stands for complex conjugation.

At $O(\varepsilon)$ the solvability conditions for ψ_1 are automatically satisfied, and thus we can solve ψ_1 as

$$\psi_1=-iA_Z\phi^{11}-2A_X\phi^a-2A_Y\phi^b+B\phi^{02}, \tag{8}$$

where $B(X,Y,Z)$ is the envelope of the second eigenfunction ϕ^{02}, $(L+\mu)\phi^a=\phi_x^{01}$, $(L+\mu)\phi^b=\phi_y^{01}$, and ϕ^a, ϕ^b are assumed to be orthogonal to ϕ^{01} and ϕ^{02}.

Now we proceed to the ψ_2 equation at $O(\varepsilon^2)$. The orthogonality condition with ϕ^{01*} is automatically satisfied, and the orthogonality condition with ϕ^{02*} gives

$$iB_Z=A_{ZX}-A_{ZY}+2A_{XX}-2A_{YY}, \tag{9}$$

which defines the connection between envelopes A and B of the two eigenmodes at the Bloch surface intersection. Under this relation, the ψ_2 equation can be solved.

Finally we proceed to the ψ_3 equation at $O(\varepsilon^3)$. The orthogonality condition with ϕ^{01*} gives

$$\begin{aligned}&\partial_Z^3A-8(\partial_X^2+\partial_Y^2)\partial_ZA-8(\partial_X^2-\partial_Y^2)(\partial_X-\partial_Y)A\\&\quad+8(\partial_X^2-\partial_Y^2)(iB)+\alpha\partial_ZA+i\tilde{\sigma}|A|^2A=0,\end{aligned} \tag{10}$$

where

$$\alpha=2V_0^2\eta,\qquad \tilde{\sigma}=-i\sigma\frac{\int_0^{2\pi}\int_0^{2\pi}|\phi^{01}|^2\phi^{01}\phi^{21}\mathrm{d}x\mathrm{d}y}{\int_0^{2\pi}\int_0^{2\pi}\phi^{01}\phi^{21}\mathrm{d}x\mathrm{d}y}.$$

This equation, combined with Eq. (9), yields a single fourth-order envelope equation for A as

$$\begin{aligned}&\partial_Z^4A-8(\partial_X^2+\partial_Y^2)\partial_Z^2A+16(\partial_X^2-\partial_Y^2)^2A\\&\quad+\alpha\partial_Z^2A+i\tilde{\sigma}\partial_Z(|A|^2A)=0.\end{aligned} \tag{11}$$

It remains to relate the initial conditions for ψ with those for envelope Eq. (11). By collecting the ψ_0, ψ_1 and ψ_2 solutions from the above analysis and projecting the resulting perturbation series solution in Eq. (6) onto the eigenfunctions and generalized eigenfunctions, we find the dominant terms of Ψ are given by

$$\Psi\approx\varepsilon^{\frac{3}{2}}(A\phi^{01}+\epsilon B\phi^{02}+\epsilon C\phi^{11}+\epsilon^2D\phi^{21}), \tag{12}$$

where

$$C=-i(A_Z+2A_X+2A_Y), \tag{13}$$

$$D=-A_{ZZ}-2A_{ZX}-2A_{ZY}-\frac{\alpha}{2}A+4iB_X-4iB_Y. \tag{14}$$

Thus, from the initial envelope functions A, B, C, D of the eigenfunctions and generalized eigenfunctions in Ψ, we can obtain initial conditions for A, A_Z, A_{ZZ} and A_{ZZZ} from Eqs. (10), (13), and (14).

The envelope Eq. (11) reveals important physical features of the envelope dynamics, and its solutions strongly agree with those in Eq. (1), as we will elaborate below. For demonstration purposes, we take the initial conditions

$$\begin{aligned}&A=A_0e^{-(X^2+Y^2)},\qquad A_Z=A_{ZZ}=0,\\&\partial_Z^3A=-i\tilde{\sigma}|A|^2A,\end{aligned} \tag{15}$$

in the envelope equation, or the equivalent initial conditions based on Eq. (12) for simulations of Eq. (1). For the constants we take $V_0^2=6$, $\epsilon=0.1$, and $\eta=0$ or 1 (at or below phase transition, respectively). Then we find $\alpha=12\eta$, and $\tilde{\sigma}\approx 7.3\sigma$.

In the linear equation at the phase transition point, i.e., $\sigma=\tilde{\sigma}=0$, Eq. (11) has the general solution

$$\begin{aligned}A=&A_1(X-2Z,Y-2Z)+A_2(X-2Z,Y+2Z)\\&+A_3(X+2Z,Y-2Z)+A_4(X+2Z,Y+2Z)\end{aligned} \tag{16}$$

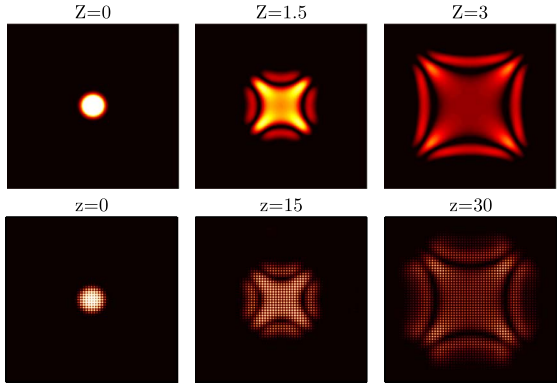

Fig. 2. Pyramid diffraction of a Gaussian wavepacket in the linear equation below phase transition. (Upper row) Diffraction in the envelope Eq. (11). (Lower row) Diffraction in full Eq. (1).

for arbitrary A_n functions (these A_n functions can be readily related to the initial conditions of A, A_Z, A_{ZZ} and A_{ZZZ}). In general, this solution corresponds to an expanding square wave front propagating with speeds ± 2 in both X and Y directions, which we term pyramid diffraction. For the initial condition in Eq. (15), this pattern is illustrated in Fig. 1 for both the envelope and full equations. Using the explicit formula of A_n for this initial condition, the fine structure in this diffraction pattern (such as the formation of dark lines) can also be explained.

In the linear equation but below the phase transition point ($\alpha = 12$, $\tilde{\sigma} = 0$), the pyramid diffraction is qualitatively similar to that in Fig. 1, with wave fronts expanding roughly like a square. But the wave fronts are no longer flat. In addition, the core develops an "x" shape. An example is shown in Fig. 2, where diffractions in both the envelope and full equations are displayed.

In the presence of nonlinearity ($\tilde{\sigma} \approx 7.3\sigma$) and below phase transition, the wave packet diffracts away if its initial amplitude is below a certain threshold value. This nonlinear diffraction is also pyramid-like, closely resembling the linear pyramid diffraction in Fig. 2. An example is displayed in Fig. 3 (upper left panel). However, if the initial amplitude is above this threshold, the envelope solution blows up to infinity in a finite distance. For example, with the initial condition in Eq. (15), the envelope solution in Eq. (11) blows up when $A_0 > 3.2$. These blowup solutions are displayed in Fig. 3 (upper middle and right panels). Remarkably, this blowup is independent of the sign of the nonlinearity, a fact which is clear from the envelope Eq. (11), since a sign change in $\tilde{\sigma}$ can be accounted for by taking the complex conjugate of this equation. In Eq. (1), we have confirmed that similar growth occurs for both signs of the nonlinearity as well (see Fig. 3, lower row). In both cases, solutions rise to very high amplitudes as the envelope equation predicts. This insensitivity of the envelope dynamics to the sign of nonlinearity strongly contrasts the one-dimensional case [14] and is surprising.

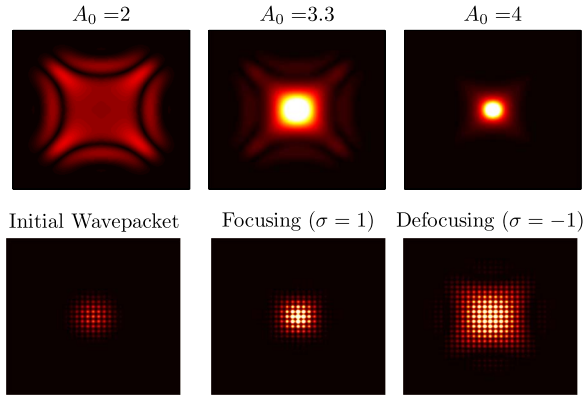

Fig. 3. Nonlinear dynamics of wave packets below phase transition. (Upper row) Envelope solutions in Eq. (11) at $Z \approx 2$ for three values of A_0 in (15). (Lower row) Solutions of Eq. (1) for the initial wavepacket with $A_0 = 6$ (left) at later distances under focusing (middle) and defocusing (right) nonlinearities.

In summary, we have analyzed nonlinear dynamics of wave packets in two-dimensional $\mathcal{PT}$-symmetric lattices near the phase transition point. In the linear regime, pyramid diffraction is demonstrated. In the nonlinear regime, wave blowup is obtained for both focusing and defocusing nonlinearities.

This work is supported in part by AFOSR.

References

1. C. Bender and S. Boettcher, Phys. Rev. Lett. **80**, 5243 (1998).
2. A. Ruschhaupt, F. Delgado, and J. G. Muga, J. Phys. A: Math. Gen. **38**, L171 (2005).
3. R. El-Ganainy, K. G. Makris, D. N. Christodoulides, and Z. H. Musslimani, Opt. Lett. **32**, 2632 (2007).
4. A. Guo, G. J. Salamo, D. Duchesne, R. Morandotti, M. Volatier-Ravat, V. Aimez, G. A. Siviloglou, and D. N. Christodoulides, Phys. Rev. Lett. **103**, 093902 (2009).
5. C. E. Rueter, K. G. Makris, R. El-Ganainy, D. N. Christodoulides, M. Segev, and D. Kip, Nat. Phys. **6**, 192 (2010).
6. A. Regensburger, C. Bersch, M. A. Miri, G. Onishchukov, D. N. Christodoulides, and U. Peschel, Nature **488**, 167 (2012).
7. R. Driben and B. A. Malomed, Opt. Lett. **36**, 4323 (2011).
8. I. V. Barashenkov, S. V. Suchkov, A. A. Sukhorukov, S. V. Dmitriev, and Y. S. Kivshar, Phys. Rev. A **86**, 053809 (2012).
9. Z. H. Musslimani, K. G. Makris, R. El-Ganainy, and D. N. Christodoulides, Phys. Rev. Lett. **100**, 030402 (2008).
10. S. Longhi, Phys. Rev. Lett. **103**, 123601 (2009).
11. K. G. Makris, R. El-Ganainy, D. N. Christodoulides, and Z. H. Musslimani, Phys. Rev. A **81**, 063807 (2010).
12. Z. Lin, H. Ramezani, T. Eichelkraut, T. Kottos, H. Cao, and D. N. Christodoulides, Phys. Rev. Lett. **106**, 213901 (2011).
13. S. Nixon, L. Ge, and J. Yang, Phys. Rev. A **85**, 023822 (2012).
14. S. Nixon, Y. Zhu, and J. Yang, Opt. Lett. **37**, 4874 (2012).